International Journal of Pharmaceutics 592 (2021) 120100

Contents lists available at ScienceDirect

International Journal of Pharmaceutics

journal homepage: www.elsevier.com/locate/ijpharm

Solid lipid nanoparticle-loaded mucoadhesive buccal films – Critical quality attributes and *in vitro* safety & efficacy

Martina M. Tzanova [a,*], Ellen Hagesaether [b], Ingunn Tho [a]

[a] Department of Pharmacy, University of Oslo, Norway
[b] Faculty of Health Sciences, Oslo Metropolitan University, Norway

ARTICLE INFO

Keywords:
Polymeric films
Lipid carrier
Coumarin 6
Permeability
Toxicity
HT29-MTX cells

ABSTRACT

The objective of this work was to develop and characterize solid lipid nanoparticle (SLN)-loaded mucoadhesive films to reveal their potential as successful drug formulations. SLNs based on lipid (Lipoid S100) and surfactant (polysorbate 80) were prepared using the solvent-injection method, and their properties examined using experimental designs. Further, the marker coumarin 6 (C6) was solubilized in the particles as a model for a lipophilic drug. Lipid and surfactant concentrations influenced the particle size, while C6 had minor impact. The particle size distribution was narrow and the storage stability satisfactory for 4 months (4 °C). The incorporation of the nanoparticles into a film matrix consisting of HPMC and glycerol, increased film thickness and flexibility, and slightly decreased the mechanical strength. The mucin interaction and disintegration time of the films were unimpaired. Film uniformity was satisfactory. Solubilisation in SLNs reduced the rate and extent of permeation of C6 through a monolayer of mucus-producing HT29-MTX cells. When the particles were incorporated into the mucoadhesive film, this effect was compensated for. In conclusion, this project was a first step in the successful development of an SLN-loaded mucoadhesive film formulation and served its purpose in revealing the formulation's uniformity, mucoadhesiveness and biocompatibility.

1. Introduction

Poorly water-soluble drugs pose a challenge for the formulation scientist. Amongst the many approaches to drug solubilisation, the use of lipid-based nanoparticles has emerged as an attractive one. Solid lipid nanoparticles (SLNs) are lipid-based colloidal drug delivery systems consisting of a solid lipid core surrounded by one or more surfactants as stabilizing agents. (Geszke-Moritz and Moritz, 2016; Gordillo-Galeano and Mora-Huertas, 2018). SLN are well-tolerated and able to solubilize and protect drugs (Douroumis and Fahr, 2012; Geszke-Moritz and Moritz, 2016). According to the literature, SLNs are usually stable for over a year, when stored properly (Geszke-Moritz and Moritz, 2016).

The evident lack of appropriate medicines for children, and the fact that the majority of paediatric treatments involve off-label use and unlicensed drugs, have led to a global emphasis on improving paediatric accessibility to approved medicinal products (European Medicines Agency, 2006). Mucoadhesive films for buccal administration are a solid dosage form with excellent patient acceptability. Additionally, hepatic first-pass metabolism and pre-systemic elimination in the GI-tract are avoided. The formulation can be removed, if necessary. Such a dosage form could also be administered to unconscious patients as a less invasive alternative to the usual parenteral routes of administration.

Earlier, various types of nanoparticles have been studied in polymeric film formulations, e.g. insulin-encapsulating chitosan nanoparticles have been loaded in chitosan films (Mortazavian et al., 2014), nystatin-encapsulating PLA, PLGA and alginate nanoparticles have been loaded in HPMC films (Roque et al., 2018), chitosan films have been impregnated with peptide-encapsulating PEG-b-PLA nanoparticles (Giovino et al., 2013), curcumin-encapsulating chitosan coated PCL nanoparticles have been loaded in chitosan films (Mazzarino et al., 2014), melatonin-encapsulating microparticles have been loaded in maltodextrin orodispersible films (Musazzi et al., 2019) and vitamin B6-encapsulating liposomes have been loaded in SCMC-HPMC films (Abd El Azim et al., 2015), all for buccal use. A few reports describing preparations based on the idea of incorporating SLNs in formulations for buccal administration have also been published in the recent years – coumarin-loaded SLNs in lyophilized sponges (Hazzah et al., 2015) and didanosine-loaded SLNs in monolayer multipolymeric films (Jones et al., 2014). SLNs have been reported as a taste-masking strategy (Walsh et al., 2014), and loading in polymeric mucoadhesive films can allow for

* Corresponding author at: Department of Pharmacy, Faculty of Mathematics and Natural Sciences, P.O.Box 1068 Blindern, 0316 Oslo, Norway.
E-mail address: martina.tzanova@farmasi.uio.no (M.M. Tzanova).

https://doi.org/10.1016/j.ijpharm.2020.120100
Received 11 June 2020; Received in revised form 28 October 2020; Accepted 15 November 2020
Available online 21 November 2020

a prolonged residence time on the buccal mucosa. The apparent advantages of using SLNs above the more commonly employed polymeric nanoparticles is their superior ability to solubilize lipophilic drugs and great biocompatibility, especially when phospholipids are utilized (Geszke-Moritz and Moritz, 2016).

The aim of this project was to lay the groundwork for the development of an SLN-loaded mucoadhesive film formulation, which would allow the solubilisation of poorly water-soluble drugs, as well as provide taste masking; hence, targeting the paediatric population. SLNs consisting of a phospholipid (Lipoid S100) and a surfactant (polysorbate 80) were prepared using the affordable and straightforward solvent-injection method. The properties of the nanoparticles were examined using experimental designs. Of interest was also the solubilisation of the poorly water-soluble model substance coumarin 6 (C6). Special focus was on how the presence of nanoparticles influenced the critical quality attributes of the films, such as uniformity, mechanical properties and mucin interaction. Finally, the mucoadhesiveness and biocompatibility, as well as permeability of C6 from different formulations, were studied using monolayers of differentiated, mucus-producing HT29-MTX cells.

2. Materials and methods

2.1. Materials

Lipoid S100 (soybean phosphatidylcholine, $\geq$ 94% pure) was generously supplied by Lipoid GmbH (Ludwigshafen, DE). Glycerol (Glycerolum (85 per centum)) was purchased from Den norske eterfabrikken (A-Pro AS) (Oslo, NO). Hydroxypropyl methylcellulose 5 (η = 5 mPa·s for a 1% (w/w) solution at 25 ℃; HPMC) was purchased from NMD (Oslo, NO). Coumarin 6 (98% pure; C6), 5(6)-carboxyfluorescein (CF), Hank's balanced salt solution (HBSS), mucin from porcine stomach (type II), Dulbecco's Modified Eagle's Medium with high glucose (DMEM), inactivated fetal bovine serum (FBS), penicillin (100 units/mL), streptomycin (100 µg/mL) (Pen-Strep), non-essential amino acids (NEAA) and trypsin-EDTA solution were purchased from Sigma-Aldrich (Saint Louis, MO, USA). Methanol (analytical grade) was purchased from VWR International, LLC (West Chester, PA, USA). Potassium dihydrogen phosphate (KH_2PO_4), disodium hydrogen phosphate dihydrate ($Na_2HPO_4{\cdot}2H_2O$), sodium dihydrogen phosphate monohydrate ($NaH_2PO_4{\cdot}H_2O$) and Tween® 80 (polysorbate 80; PS80) were purchased from Merck (Darmstadt, DE). The cell line HT29-MTX was kindly provided by Dr. Thécla Lesuffleur (INSERM UMR S 938, Paris, FR).

2.2. Solutions

2.2.1. Phosphate-buffered saline (PBS) pH 7.4

Prepared from tablet (Sigma Aldrich, Saint Louis, MO, USA) dissolved in 200 mL Milli-Q water (Millipore Q-Pod® with 0.22 µm Millipak® Express 40 filter; Merck Millipore, Darmstadt, DE)

2.2.2. Phosphate buffer (PB) pH 7.4

Solutions A (9.073 g/L KH_2PO_4 in Milli-Q water) and B (11.87 g/L $Na_2HPO_4{\cdot}2H_2O$ in Milli-Q water) were mixed in a ratio 19.7:80.3 to obtain a buffer solution of pH 7.4 (FiveEasy pH/mV meter; Mettler Toledo Inc., Columbus, OH, USA).

2.2.3. Phosphate buffer (PB) pH 6.8

0.297 g $Na_2HPO_4{\cdot}2H_2O$ and 0.459 g $NaH_2PO_4{\cdot}H_2O$ were dissolved in Milli-Q water and diluted to 1000.0 mL of the same solvent; pH was adjusted before dilution.

2.2.4. Cell culturing media

The cell culturing media was prepared by enriching DMEM, containing L-glutamine, sodium pyruvate and phenol red with a range of 6.8–7.2 (sodium bicarbonate buffer) with 10% (v/v) FBS, 1% (v/v) Pen-Strep and 1% (v/v) NEAA.

2.3. Methods

2.3.1. Preparation of solid lipid nanoparticles

A modified version of the solvent-injection method as proposed by Ternullo et al. (2017) was employed. Briefly, the required amount of Lipoid S100 was dissolved in methanol or a 50 µg/mL methanolic C6 solution (for "placebo" (S1 – S13) and C6-loaded particles, respectively). The aqueous phase (6 mL) was prepared by appropriately diluting a 10 mg/mL stock solution of PS80 in PBS or using pure PBS. It was stirred at 300 rpm as 2 mL (3 mL Soft Ject® syringe, Luer Slip tip, Henke Sass Wolf, Tuttlingen, DE) of the lipid solution was rapidly injected into it via a Sterican® needle (0.3 × 12 mm), the needle almost touching the surface. The suspension was allowed to stir (300 rpm) for 2 h at ambient temperature and was thereafter refrigerated (4 ℃) overnight, prior to particle size reduction.

The methanol (2 mL) was evaporated by bubbling N_2 gas through the suspension for about 15 min, the vial immersed in a water bath at 40 – 45 °C.

For the particle size reduction, a hand-extrusion method was employed, utilizing 10 mL Luer Lock tip syringes (Henke Sass Wolf, Tuttlingen, DE), Swinnex® non-sterile filter holder (EMD Millipore Corporation, Billerica, MA, USA) and Whatman® Nuclepore Track-Etch polycarbonate membranes (pore size: 0.8, 0.4 or 0.2 µm; GE Healthcare, Maidstone, UK). The extrusion took place in a stepwise manner through membrane filters of descending pore sizes – 0.8, 0.4 and 0.2 µm. The extruded suspension was refrigerated, prior to the particles' characterization.

2.3.2. Characterization of solid lipid nanoparticles

2.3.2.1. Particle size, distribution and zeta potential. The intensity-mean hydrodynamic diameter and particle size distribution (z-average (nm) and PdI, respectively) of each formulation were measured the day after extrusion, using backscatter (angle: 173) dynamic light scattering (DLS) on Zetasizer Nano-ZS (Malvern Instruments, Oxford, UK). SLN-suspension was diluted 1:100 with 0.2 µm filtrated PBS directly into a disposable polystyrene cuvette for Zetasizer (Sarstedt AG & Co., Nümbrecht, DE) right before insertion into the instrument. Before measurement, the samples were equilibrated at 25 °C for 300 s, and each sample was measured in triplicate. Attenuator value was chosen automatically and was between 6 and 8 for all measurements.

The zeta potential (mV) was measured using a dip cell and the laser Doppler micro-electrophoresis principle on the Zetasizer. Calibration was performed with Malvern Zeta potential transfer standard (−42 ± 4.2 mV). The samples were prepared as described earlier, in both water and PBS. Samples were equilibrated at 25 °C for 120 s, and each sample was measured in triplicate.

2.3.2.2. Measurement of total amount of C6 in SLN formulations. In order to quantify C6 in the particle suspensions, the particles were dissolved by diluting an aliquot of the suspension 1:100 with methanol. Complete particle dissolution was confirmed with DLS measurements. The fluorescent intensity (FI) of the samples was measured in triplicate on a black, flat-bottom uncoated 96-well plate (VWR International, LLC, West Chester, PA, USA) on a CLARIOstar® Microplate reader (equipped with MARS Data Analysis Software, BMG LABTECH GmbH, Ortenberg, DE) with an excitation wavelength, λ_{ex} = 454 nm and emission wavelength, λ_{em} = 509 nm. Gain and focal height were chosen automatically by the instrument. Total C6 was quantified based on a calibration curve in methanol ($R^2 \geq 0.999$). In addition, specific calibration curves were obtained for other relevant solvent compositions, applying the corresponding instrumental settings, all with $R^2 \geq 0.998$.

2.3.2.3. Storage stability. The stability of the particle suspensions was evaluated by measuring the particle size and its distribution over time,

at first once a week for the first 4 weeks, then once a month for 4 months. All formulations were stored refrigerated (4 °C) under an inert atmosphere (N_2 gas) in sealed injection vials.

2.3.3. Multivariate experimental design

For design of experiments (DoE) and multivariate data analyses, The Unscrambler® version 9.8 (Camo ASA, Trondheim, NO) was utilized.

2.3.3.1. Screening and optimization of formulation and process parameters. For comparison purposes, a batch of SLNs (S1) was prepared by the general procedure described earlier, with a final lipid concentration of 30 mg/mL and no surfactant. Further, three factors of interest: lipid concentration (A), surfactant concentration (B) and number of extrusion cycles per membrane pore size (C), were analysed using a two-level fractional factorial design (i.e. 2^{3-1}) with three centre points (CP). The design had resolution III so that all main effects were confounded with two-factor interactions.

Based on the findings from the screening design, a central composite-like design (CCD) was set up to further investigate the effects of lipid (A) and surfactant (B) concentrations on the particle size and polydispersity, while keeping the number of extrusion cycles constant at 3. The cube points, S2 and S3, from the screening design were kept and the star points were chosen at distance 1.2 from the centre point. An overview of all formulations prepared as a part of both experimental designs is given in Table 1.

2.3.3.2. Data analysis. The effects (linear and non-linear) of the design variables and their interactions on the response variable particle size (nm) were evaluated separately for each design, using multiple linear regression (MLR). Prior to the analysis, the design variables were normalized and returned back to their actual values for obtaining a relevant response surface plot once a statistically significant model was obtained. Uncertainty of the regression coefficients was estimated by analysis of variance (ANOVA). A more detailed description of these methods is given by Esbensen et al., 2001.

2.3.4. Preparation of films

Films were prepared by the solvent casting method. Film matrix, consisting of 8% (w/w) HPMC, 2% (w/w) glycerol and PB pH 7.4 as solvent, was prepared by wetting the polymer with glycerol and gradually adding the solvent under stirring (Adrover et al., 2018). The polymer dispersion was then allowed to stir for at least 4 h. For SLN-loaded films, 5% (w/w) of an SLN-suspension was added to the film matrix, by one of two methods – "bolus" or "coating" – and the mixture was allowed to stir for additional 4 – 5 h. When using the "bolus" method, the correct mass of the suspension was added all at once to the premixed polymeric film matrix. For the "coating" method, the proper amount of an SLN-suspension was weighed into a beaker, diluted with some of the solvent and a concentrated film matrix (HPMC: 12% (w/w), glycerol: 3% (w/w)) was added dropwise under constant stirring. In both cases, care was taken to remove any foam from the surface of the mixture prior to film casting.

Films were cast on a release liner of cellophane (Panduro AS, Gressvik, NO) on a levelled glass plate on the Coatmaster 510 (Erichsen GmbH & Co. KG, Hemer, DE) using a casting knife with a gap opening of 1000 μm (Film Applicator System Wasag Model 288, Erichsen, DE). Other casting parameters: speed = 20 mm/s, path = 400 mm. The film was allowed to dry overnight at ambient conditions (temperature and relative humidity (RH)). The dry film sheet was cut into single-dose units with dimensions of 2.0 × 2.0 cm. The single-dose film units were stored in a desiccator, with RH range 33.2 – 33.6% (oversaturated $MgCl_2{\cdot}6H_2O$ solution in water) at room temperature for 7 days before further tests were conducted. The aim was to ensure that humidity fluctuations and differences between samples would not influence the mechanical properties of the films.

A summary of all investigated film formulations is given in Table 2.

2.3.5. Characterization of films

2.3.5.1. Mass and film thickness. Depending on the batch size, 10 – 20 single-dose units were selected at random, weighed one by one and their thickness was measured at five points using a manual micrometre (Cocraft 0 – 25 mm ± 0.04 mm; Clas Ohlson, SE). The uniformity of mass was evaluated according to Ph. Eur. monograph *2.9.5 Uniformity of mass of single dose preparations* for *Tablets (uncoated or film coated; average mass <80* mg), as the closest dosage form (European Pharmacopoeia Commission, 2018).

2.3.5.2. Puncture test. Film samples with known mass and thickness were subjected to a puncture test – 10 or 20 units per film formulation –

Table 1
Overview of SLN formulations prepared, design these belong to (reference/no design, 2^{3-1} with centre point screening and central composite-like design) and each formulation's basic characteristics. Results are given as a mean of three measurements ± SD *or* a mean value of several formulation batches (where available).

Formulation	Formulation parameters A (Lipoid S100; mg/mL)	B (Polysorbate 80; mg/mL)	C (№ of extrusions)	Design/Type *	Particle characteristics Z-average (nm)	PdI
S1	30	0	3	reference	175 ± 1	0.166 ± 0.014
S2	30	1	3	2^{3-1}	137 ± 1	0.098 ± 0.008
S3	10	10	3		99 ± 1	0.114 ± 0.010
S4	10	1	7		102 ± 0	0.162 ± 0.004
S5	30	10	7		120 ± 0	0.104 ± 0.002
S6 (n = 3)	20	5.5	5		124 ± 2 **	0.102 ± 0.016 **
S7	10	1	3	CCD	119 ± 10 **	0.149 ± 0.019 **
S8	30	10			127 ± 1 **	0.099 ± 0.005 **
S9 (n = 3)	20	5.5			128 ± 3 **	0.104 ± 0.003 **
S10	8	5.5			111 ± 1	0.119 ± 0.012
S11	20	10.9			123 ± 1	0.075 ± 0.019
S12	32	5.5			142 ± 1	0.112 ± 0.006
S13	20	0.1			163 ± 1	0.104 ± 0.012
S2-C6	30	1		C6-loaded	149 ± 0	0.094 ± 0.012
S3-C6	10	10			107 ± 1	0.090 ± 0.013
S7-C6	10	1			121 ± 7 **	0.150 ± 0.004 **
S8-C6	30	10			125 ± 1	0.091 ± 0.003
S9-C6	20	5.5			134 ± 4 **	0.137 ± 0.072 **

* 2^{3-1}: two-level fractional factorial screening design; CCD: central composite-like optimisation design; C6-loaded: SLNs loaded with coumarin 6, not part of a multivariate experimental design.

** Results are a mean value for several batches (n ≥ 2).

Table 2
Overview of film formulations with their corresponding average mass, thickness, puncture strength and elongation to break (values are given as mean ± SD).

Formulation	SLN addition method ("bolus"/"coating")	Type of SLN	Unit mass (mg)	Thickness (μm)	Puncture strength (N/mm^2)	Elongation to break (%)
F1	–	none	48.05 ± 2.18 *	99.3 ± 5.0	1.07 ± 0.11	8.73 ± 1.32
F2	bolus	S7	58.39 ± 3.69 **	113.1 ± 6.6	1.07 ± 0.06	9.01 ± 2.36
F3	coating		54.29 ± 2.79 **	105.6 ± 6.3	0.97 ± 0.07	9.17 ± 2.43
F4	bolus	S8	56.95 ± 3.89 **	117.9 ± 7.9	0.97 ± 0.03	8.54 ± 2.27
F5	coating		53.72 ± 4.24 **	109.5 ± 8.1	0.92 ± 0.06	8.94 ± 2.35
F6	coating	S9-C6	50.49 ± 4.13 ***	103.0 ± 8.0	N/A	N/A

* n = 20, ** n = 10 and *** n = 15; N/A = not available.

using a texture analyser TA-XT Plus (with Exponent software, Stable Micro Systems Ltd, Godalming, Surrey, UK).

This test was a modification of an earlier published method (Preis et al., 2014). Briefly, a single-dose unit of a film (2 × 2 cm) was mounted in the sample holder. A flat cylindrical probe (r_{probe} = 3.52 mm, A_{probe} = 38.8 mm^2) was lowered into the sample holder opening (r_{sample} = 6.985 mm) with a speed of 2.0 mm/sec (pre-test speed) until it touched the film (trigger force 5 g = 0.049 N), and the speed was reduced to 0.1 mm/sec (test speed) until the film piece punctured. Puncture force (N) and distance travelled by the probe from the trigger force until film rupture (i.e. the penetration depth, *b*; mm) were used to calculate puncture strength (tensile strength; N/mm^2) and elongation to break (%) according to the following equations, respectively:

$$Tensile\ strength\left(\frac{N}{mm^2}\right) = \frac{Puncture\ force\ (N)}{A_{probe}(mm^2)} \quad (1)$$

$$Elongation\ to\ break(\%) = \left(\frac{\sqrt{a'^2 + b^2} + r_{probe}}{r_{sample}} - 1\right) \times 100 \quad (2)$$

where *a'* ($= r_{sample} - r_{probe}$) is the initial length of the sample that is not punctured by the probe.

2.3.5.3. Disintegration time: Petri dish method. Single-dose units of a reference film (containing no SLN) and an SLN-loaded film (n = 3 for each) were placed in Petri dishes (VWR International, LLC, West Chester, PA, USA) and 30 mL preheated (37 °C) PBS pH 7.4 was poured over them. The dishes were placed in a shaking incubator (Environmental Shaker-Incubator ES-20; Biosan, Riga, LV) at 37 °C and 60 rpm. The time until complete dissolution and no visible traces of coherent film matrix was recorded for each film unit.

2.3.5.4. Residual moisture content: Loss on drying. Single-dose units of a reference and SLN-loaded films (n = 3 for each) were placed in individual, pre-weighed porcelain crucibles and weighed. The crucibles were placed into a silica gel-filled desiccator, which was placed inside a laboratory drying oven (Series 9000, Termaks A/S, Bergen, NO) at 50 °C for 96 h to remove all residual moisture. Upon termination of the experiment, the desiccator was closed rapidly to avoid moisture absorption, and allowed to reach room temperature prior to gravimetric determination of the loss on drying.

2.3.5.5. Dose uniformity: C6 quantity throughout the film. Single-dose units of SLN-loaded film (n = 5) were dissolved separately in 2 mL of buffer, and an aliquot was diluted 1:100 in methanol. The solution was quantified as described for the SLN-suspensions.

2.3.5.6. In vitro mucin interaction test. This test was a modified version an earlier published method (Hagesaether et al., 2009). Briefly, a square film sample (1.0 × 1.0 cm) was placed between two wetted pieces (2.0 × 2.0 cm) of filter paper with inert backing coat (Watman® Benchkote, St. Louis, MO, USA), attached to the bottom stationary glass plate and the upper moving, homemade flat probe (11 × 11 cm) with the help of double-sided adhesive tape. 50 μL of either a PB pH 6.8 (estimating the unspecific adhesion) or mucin 3% (w/w) dispersion in the same buffer (estimating the general mucoadhesion) were applied to each of the two filter paper pieces immediately before a film sample was introduced. The test was initiated at once to ensure even moistening of the film from both sides. Pre- and post-test speeds were set to 1.0 and 10 mm/sec, respectively. When the two surfaces came in contact (trigger force 5 g = 0.049 N), a force (preload) of 200 g was applied for 100 sec by the mobile part, followed by retraction at a speed of 0.01 mm/sec (test) until a complete detachment of the two surfaces. Adhesive force (i.e. peak force, F_{max}, N) and work of adhesion (i.e. area of work, *AUC*, N × mm) were recorded. Only F_{max} was used to calculate the estimated mucin interaction as the difference between the average F_{max} of general mucoadhesion and the unspecific adhesion. For each medium, 10 film samples were measured, i.e. a total of 20 samples per formulation. The film thickness (middle point) of each film piece was measured before the test.

2.3.6. Cell studies

2.3.6.1. Cell culturing and seeding. A vial of passage number 26 (P26) of HT29-MTX cells was thawed, seeded, incubated at 37 °C and an atmosphere of 5% CO_2 and passaged at 70 – 90% confluency (with trypsin-EDTA solution) three times before being seeded (P30; seeding density: 2.4×10^4 cells/cm^2) for the experiments. The cells were cultured for 21 – 23 days before the experiments were carried out. The medium was changed every second day for the maintenance in cell culturing flasks (CellBIND® surface treated, U-shaped T75; VWR International, LLC, West Chester, PA, USA) and at least every second day in the experimental plates.

For the mucoadhesion study, cells from P30 were seeded with a density of 2.4×10^4 cells/cm^2 onto a black optical bottom polystyrene 96-well plate (cell culture dish; Nunclon™, Thermo Fischer Scientific, Waltham, MA, USA) with a growth area of 0.36 cm^2 per well.

For the permeability study, cells the same passage and at the same seeding density were seeded in 6-well flat-bottom plates (Nunclon™, Nunc A/S, DK) on Transwell® cell culture inserts with 0.4 μm PET membranes with growth area of 4.2 cm^2 (Falcon®, Corning Inc., Durham, NC, USA).

In order to evaluate the integrity of the cell monolayer, the transepithelial electric resistance (TEER; Ω) was measured in the Transwell® setup once daily, using a Millicell® ERS-2 Voltohmmeter (Millipore Co, Bedford, MA, USA), and before and after the cells' exposure to formulations as a part of the permeability study. Values were expressed as unit area resistance, i.e. Ω × cm^2, as a standardised unit of resistance. Resistance from the inserts themselves (blank resistance) was subtracted before standardizing.

2.3.6.2. In vitro mucoadhesion. This novel approach was proposed by Adamczak *et al.*, and is based on measuring the amount of a fluorophore adhering to a monolayer of a differentiated HT29-MTX cell-layer in a 96-well plate (Adamczak et al., 2016). For standardisation purposes, the initial fluorescent intensity (F_0) of each formulation (V = 200 μL; n

varied) was measured on a black optic bottom 96-well plate in a similar fashion as the samples.

Cell monolayers were washed a couple of times with HBSS, before incubation with 200 μL samples in a shaking incubator at 37 °C and 60 rpm for one hour. The supernatants were then carefully removed. FI was measured directly on the cell monolayers before (F_{C1}), and after (F_{C2}) they were washed with 200 μL of HBSS.

Film samples (F6) were prepared in one of two ways – as dry film pieces ($A = 0.25$ cm^2; n = 5) and as dissolved film pieces ($A = 4.0$ cm^2; n = 5). The dry film pieces (0.5 × 0.5 cm) were carefully placed directly on the cell monolayer (one per well) and 200 μL HBSS was pipetted over. Otherwise, a single-dose unit (2.0 × 2.0 cm; n = 5) was dispersed in 1000 μL HBSS and 200 μL aliquots from this dispersion were applied to the cell monolayers (n = 3; total number of wells = 5 × 3 = 15). The mucoadhesiveness of SLN formulation S9-C6 (corresponding to the formulation film F6 was loaded with) was also investigated by diluting 1:100 in HBSS before application (V = 200 μL; n = 5).

2.3.6.3. Permeability study. The experiment started by recording TEER values. The cell monolayers were washed several times with HBSS in order to remove the cell culture media completely. The inserts were moved to a new plate with 2.5 mL preheated 0.5% PS80-in-HBSS in each well (acceptor chamber).

The cell monolayers were incubated with four types of samples (n = 3 for each) – a C6-in-HBSS suspension (free C6), two different concentrations of an SLN suspension (S9-C6) and an SLN-loaded film formulation (F6). For the wells with free C6, 1.5 mL HBSS was applied and spiked with an appropriate (small) volume of a concentrated methanolic C6-solution similar to C6 concentration of the film samples. For the SLN-suspension samples, an aliquot of the formulation was diluted appropriately with HBSS in order to obtain a C6 concentration matching that of the film samples (sample name: S9-C6-L) and one, which was 10 times higher (sample name: S9-C6-H). 1.5 mL of diluted suspension was applied to the donor chambers. Single-dose units from the film formulation were carefully placed over the cell monolayer and 1.5 mL of HBSS were pipetted over the film piece. The plate was incubated in a shaking incubator at 37 °C and 60 rpm for a total of four hours. The donor chamber inserts were moved hourly to a new plate with 2.5 mL fresh acceptor solution.

The concentration of C6 from each acceptor chamber solution was measured as described above ($\lambda_{ex} = 454$ nm and $\lambda_{em} = 509$ nm; black polystyrene 96-well Nunclon® plate; V = 200 μL; n = 3). Calibration curve was measured simultaneously ($R^2 \geq 0.999$).

The apparent permeability coefficient, P_{app} (cm/s), was calculated based on the following equation

$$P_{app} = \frac{dQ}{dt} \times \frac{1}{C_0 A} \quad (3)$$

where dQ/dt is the rate of drug transport at steady state (ng/s; given by the slope of the linear portion ($R^2 \geq 0.99$) of the time vs cumulative concentration curve, assuming steady-state flux), C_0 is the initial donor concentration (ng/mL), and A is the area of the monolayer (=4.2 cm^2).

The flux, J, (ng/cm^2 × h) was calculated according to the following

$$J = \frac{dQ}{dt} \times \frac{1}{A} \quad (4)$$

2.3.6.4. Cytotoxicity. After the permeability experiment, the donor chambers were emptied, the cells were washed a couple of times with HBSS and placed in a new plate with fresh HBSS. In the donor chambers, 1.5 mL of a 20 μM solution of CF-in-HBSS was applied. The plate was incubated for one hour at 37 °C and 60 rpm and final TEER values were measured. Concentration of CF in the acceptor solutions was measured (n = 3) using a plate reader at $\lambda_{ex} = 485$ nm and $\lambda_{em} = 535$ nm. Results were expressed as the percentage of the applied CF that permeated the cell monolayer. Increased permeability of CF compared to the negative control (C6-in-HBSS) was interpreted as an indication of cytotoxic effects of the formulation.

2.3.7. Statistical analysis

Outlier screening was performed on all datasets where n ≥ 10. An outlier was defined as a value, which is >1.5 × IQR (interquartile range) larger than the third quartile or smaller than the first quartile. A student's *t*-test was performed to reveal statistically significant differences, where applicable. Analysis of the equality of the variance of the two datasets within each pair was performed initially, in order to determine the correct version of *t*-test to be used. Significance level α = 0.05 was used. The multivariate statistical methods are described above.

3. Results and discussion

3.1. Solid lipid nanoparticles (SLN)

SLNs with different compositions were successfully prepared by the solvent-injection method. Coumarin 6 (C6) was chosen as a model substance for a poorly water-soluble drug (insoluble in water (Biomedicals); 0.25 μg/mL (Kim et al., 2017)) with a high permeability. C6 is an orange crystalline powder with a pKa value in the range of 0.8 – 1.6, depending on the solvent composition (Finke et al., 2014). The substance has fluorescent properties, allowing for efficient quantification using multiwell plates. For the C6-loaded SLNs, the suspension would acquire a distinct yellow colour but was equally turbid or transparent as the corresponding "placebo" SLN formulation. No visible C6 precipitate was observed in the vial or on the filter after extrusion, suggesting that all of the dye was, in fact, solubilized into the lipid nanoparticles.

3.1.1. Basic characteristics of solid lipid nanoparticles

Results on SLN size and polydispersity for all formulations are summarised in Table 1. All investigated formulations were within the size range of 100 – 180 nm with corresponding PdI of 0.075 – 0.170, demonstrating a narrow size distribution owed to the stepwise extrusion during preparation. No general correlation between particle size and polydispersity values was revealed. Reference formulation S1 displayed largest hydrodynamic diameter and highest polydispersity and the presence of surfactant decreased particle size and PdI, as more homogeneous (monodisperse) particles were formed. A slight increase in size (up to about 10 nm) was observed when C6 was included (S2-C6, S3-C6, S7-C6, S8-C6 and S9-C6 compared to their respective "placebo" formulations). This small size difference can generally be considered to have a negligible effect on the properties of the particles (Leal et al., 2017).

The zeta potential of a few chosen formulations was measured and shown to be slightly negative or positive in water and PBS, respectively, the magnitude of the apparent charge in the same order as the ones reported by Ternullo et al. (2017) for the same particles. The presence of Tween 80 did not alter the zeta potential but provided sufficient steric repulsion between the particles for adequate stability, as demonstrated by the stability study we present here.

3.1.2. Multivariate evaluation of SLN: Particle size optimization

The following three factors were studied in the screening 2^{3-1} factorial design: lipid concentration, surfactant concentration and number of extrusion cycles per membrane pore size. The results from the MLR-analysis revealed that the only main effect that was statistically significant, was the lipid concentration (confounded with the less plausible interaction between the surfactant concentration and the number of extrusions). The centre points showed a good reproducibility of the preparation method (mean ± RSD = 124 nm ± 1%), reflected in the low error sum of squares (SS_{error}) calculated by the statistical analysis. There was no significant effect of increasing the number of extrusions per pore size from 3 to 7. Hence, only the effects of lipid and surfactant concentrations were examined further in the optimization

design.

A central composite design (CCD) is an optimization design, involving the addition of axial samples – samples identical to the centre points in all but one factor, for which factor two new levels were generated with one being lower than the low level (< –1) and one higher than the high level (> 1). Thus, a total of 5 levels for each factor are obtained. This allows the creation of a model that can reveal complex interactions and non-linearities (curvature) in the response up to the third degree. In the present study, only the main effects (concentrations of lipid and surfactant) were found to be of statistical significance for the resulting particle size of SLNs. Comparably low SS_{error} to the previously discussed screening design was recorded, and the repeated CP SLN formulation, S9, exhibited a similarly low variability as before – 126 ± 1.5 nm (RSD = 1%). The size of these formulations did not differ significantly from the ones prepared with 5 extrusion cycles for the screening design, further confirming that this factor was not important for the final particle size. The effects of the concentrations of the two excipients were shown to be of the same magnitude but opposite signs (normalized coefficients: $\beta_{Lipid} = 11.151$ vs $\beta_{Surfactant} = -12.407$). The lipid concentration had a positive effect on z-average (higher concentration produced larger particles), while the amount of surfactant was inversely correlated to the response variable, and higher concentrations of PS80 were required to obtain smaller particles when the lipid concentration was kept constant. Response-surface plot based on the MLR-model in Fig. 1 shows z-average as a function of the two independent variables. The nanoparticles exhibit similar sizes when prepared from combinations of the two factors that lie diagonally to one another. This implies that it would be possible to obtain the same SLN size at lower surfactant concentration by simultaneously reducing the lipid concentrations. For comparison purposes, the surfactant-free formulation, S1, gave SLN with z-average of 174 nm. Furthermore, in addition to a narrow size range, increasing the amount of lipid resulted in increased total number of nanoparticles, thus increasing the loading and solubilisation capacity of the system. Our observations are in agreement with earlier reports of the effects of lipid and surfactant concentrations on the size of solid lipid nanoparticles (Martins et al., 2012; Schubert and Müller-Goymann, 2003). The model obtained from the optimization CCD was statistically significant with a coefficient of determination, R^2, of 0.7 between the measured and predicted response values. This implies that the model should be used with caution and only to obtain an approximation of the expected z-average for excipient concentrations within the explored design space.

Since the SLN sizes ranged between 100 and 200 nm and the polydispersity around 0.1 for all combinations produced in this study, they could be regarded as within a satisfactory range as they comply with the quality attributes of mucus-penetrating particles in literature (Leyva-Gómez et al., 2018). The fact that a range of lipid and surfactant concentrations constantly yields similar particles confirms the robustness of the system, which is beneficial with respect to large-scale production. However, above a certain level of the surfactant concentration, toxicity might become an issue.

All formulations included in the multivariate analysis showed monodispersed size distribution with PdI values in the narrow range of 0.075 – 0.166. These values were considered adequate for the needs of this project and no further statistical analysis was performed on this response.

3.1.3. *Storage stability: Particle size and distribution over time*

The particle size (z-average) and PdI of each formulation were measured and recorded for 4 months. Between each measurement, the suspensions were stored refrigerated, under an inert atmosphere to retard the hydrolysis and oxidation of the phospholipid. All investigated formulations showed good stability over time and no irreversible aggregation was observed. Both z-average and its respective PdI exhibited only minor changes (up or down) which were considered to be within experimental error. Measurement of formulation S8-C6 6 weeks post-production showed no signs of particle aggregation, confirming that there is no reason to expect that the presence of C6 would significantly influence the stability of the particles over time.

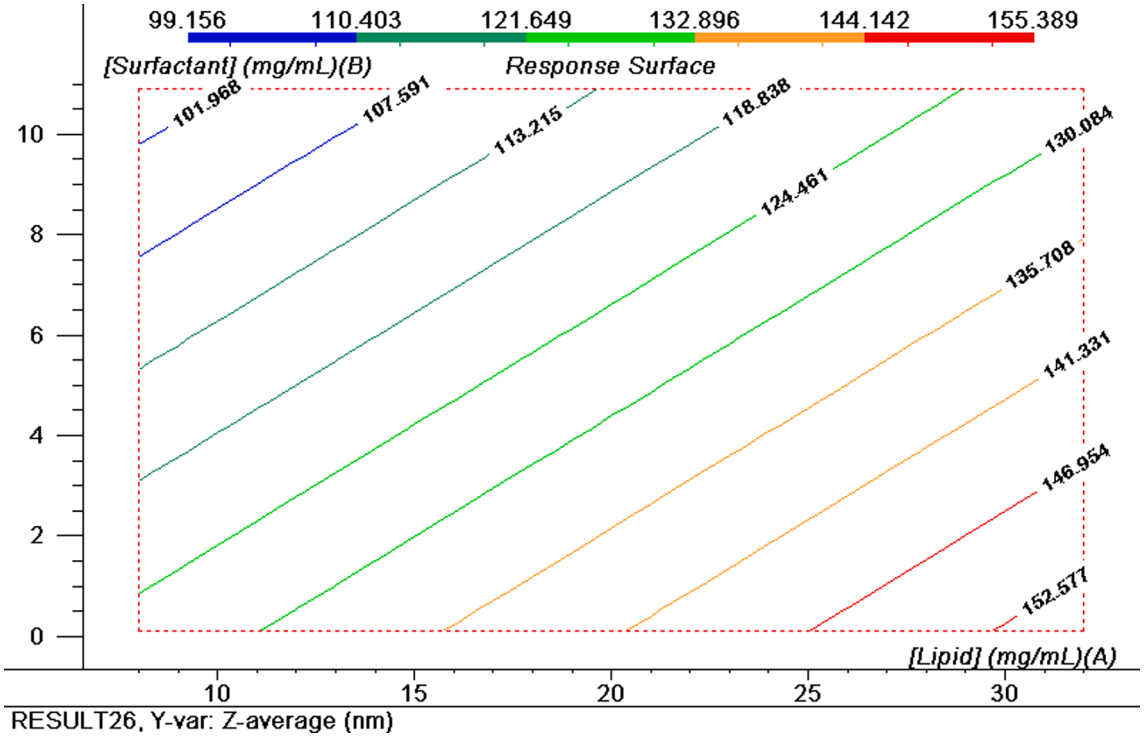

Fig. 1. Response-surface plot from MLR of the CCD showing the response variable (particle size; z-average) as a function of the concentration of lipid (x-axis) and surfactant (y-axis).

3.2. Mucoadhesive films

The films were prepared with a non-saline phosphate buffer (PB; pH 7.4), as preliminary studies showed that sodium chloride precipitated upon film drying. The reference film (no SLN) was transparent, soft and flexible. SLN-loaded films were prepared with 5% (w/w) SLN suspension. As mentioned above, the formulations containing high levels of lipid and surfactant contained a higher number of particles. Thus, even though each formulation was added 5% SLN suspension, the number of particles present in the film would be different depending on which SLN formulation was used.

The SLN suspension was added to the film matrix by two different mixing techniques and the "bolus" films seemed more turbid than the ones produced by the SLN "coating" method. This difference was more profound for the films of higher particles concentration (based on high lipid content), i.e. formulations F4 and F5. The "coating" method was inspired by the classical method for coating liposomes, where the liposomal suspension is added dropwise to a polymeric solution under stirring (Adamczak et al., 2016). Due to the viscosity of the polymer solution, addition of the polymer to the nanoparticles was preferred, aiming at coating the SLNs with HPMC. This coating would provide steric hindrance avoiding particle aggregation in the matrix and ideally, remain on the particle surface, giving the particles mucoadhesive properties upon film matrix disintegration or dissolution. Based on the macroscopic observations, the coating method seemed to prevent the SLN particles from aggregating upon film drying; thus, the less turbid appearance of the film. However, this is based solely on visual observation.

3.2.1. Characterization of films – Critical quality attributes

Relevant critical quality attributes of the films are summarized in Table 2. The single-dose units of all film formulations were in the range of approximately 45 – 60 mg with a thickness within the range of 85 – 120 μm. All studied formulations fulfilled the criteria for uniformity of mass of a solid dosage form as described for tablets in Ph. Eur. (European Pharmacopoeia Commission, 2018). Film thickness is considered to have a more significant impact on the overall mouthfeel and comfort of the patient, than the film mass. Human volunteer studies on patient acceptability of film formulations with respect to their size have shown that both films with dimensions of $2 \times 2 \times 0.1$ cm and $2 \times 3 \times 0.35$ cm have been found tolerable (Krampe et al., 2016). Considering this, any of the films proposed in the current work would be suitable for further development with respect to the film's thickness.

Regarding the uniformity of the films' thickness – well-correlated to their mass ($R \geq 0.9$) – RSD for all formulations was in the reasonably narrow range of 4 – 8%. The SLN-loaded films with a higher concentration of particles (F4 and F5, i.e. high lipid concentration) showed higher variability in thickness than the ones loaded with the lower concentration of particles (F2 and F3, i.e. low lipid concentration). Furthermore, all SLN-loaded films were thicker (6 – 19%; statistically significant at $\alpha = 0.05$) than the reference formulation F1, owing to the higher content of solid material in these formulations. Both films prepared by the "coating" method (F3 and F5) were significantly thinner than the ones prepared by the "bolus" method (F2 and F4). Finally, the SLN-loaded films were thinner than those containing polymeric micelles as a solubilisation approach (Alopaeus et al., 2020).

The disintegration behaviour of oral films is an important quality aspect of this type of formulation. An SLN-loaded film piece was the first to reach complete dissolution (7.5 min), followed closely by the reference film (8.5 min). After 10 min, the second of the parallels from both formulations had disintegrated, and after 20 min, all pieces had disintegrated. The films did not fulfil either of the compendial criteria for orodispersible formulations – USP: 30 s and Ph. Eur.: 180 s – but rather indicated that the present formulation might be better suited for a slightly longer duration of application. The results were also contradictory to the 43 s disintegration time recently reported for HPMC-films containing polymeric micelles, tested by the same method (Alopaeus et al., 2020). This can be explained by the different nature of the solubilising carriers in the two systems and difficult endpoint definition and detection for disintegration, as described in detail elsewhere (Speer et al., 2018). A prolonged contact time with the buccal mucosa is desirable for the delivery of the drug from the SLN and the mucoadhesion enables the retention of the system on the oral mucosa. It should further be noted that the disintegration time was determined in a petri dish with 30 mL fluid. Even though the fluid volume was scaled down from the compendial disintegration test, the amount would still be excessive as compared to the volume available in the oral cavity, even under stimulated salivation (Edgar et al., 2012). Hence, it is reasonable to assume that the determined disintegration times of 7.5 – 20 min, might be longer *in vivo*. Whether this is long enough for the absorption of the drug over the buccal mucosa should be subjected to further studies using an actual active pharmaceutical ingredient (API).

Residual moisture is an important parameter with respect to the mechanical properties, adhesive properties and stability of the films (Karki et al., 2016). No significant differences were found between reference and SLN-loaded films, suggesting that the presence of particles in the formulation did not affect the film's ability to retain water. Residual moisture content was on average 11% (RSD = 1%) for the reference film and 10% (RSD = 2%) for the SLN-loaded film, respectively. The values were in agreement with those reported in the literature on buccal films of a similar composition (Adrover et al., 2018; Alopaeus et al., 2020).

One of the challenges when developing new (mucoadhesive) film formulations is the lack of established and harmonized methods for determining the mechanical strength and other critical properties of the films. Two tests were employed as a part of this project – the puncture strength test, as described by Preis *et al.* (Preis et al., 2014) and the *in vitro* mucin interaction test, as described by Hagesaether *et al.* (Hagesaether et al., 2009) – in an attempt to enlighten the effect of nanoparticle incorporation on these film properties. There is no straight answer to what the puncture strength or elongation to break of a buccal film should be. Ph. Eur. declares that measures are to be taken "*to ensure that they* [mucoadhesive buccal tablets or buccal films] *possess suitable mechanical strength to resist handling without crumbling or breaking*" without specifying any further numerical values or methods to obtain these. The film should also be easy to produce homogeneously (e.g. extreme flexibility might lead to problems with reproducible cutting) in addition to effortless handling. The percentage elongation has, however, not been found to be a crucial factor, given that the films possess suitable mechanical strength (Preis et al., 2014).

In the current project, the puncture strength of reference and SLN-loaded films alike was around 1 N/mm^2 (Table 2). This is very similar to the results obtained by Alopaeus *et al.* for a film of a similar composition, is comparable to that for a commercially available film for oromucosal administration and higher than films utilizing an alternative solubilisation approach (Alopaeus et al., 2020). The values for elongation to break were within a narrow range of 8.5 – 9.2% for SLN-loaded film formulations and all these were of the same order of magnitude as the reference film (8.7%). No statistically significant correlations between film thickness and puncture strength or elongation to break were found.

Mucoadhesion is a complex phenomenon involving the wetting of the polymer and its consecutive interactions with mucus. The approach taken in this test was to isolate the adhesion resulting from the polymer's interaction with mucin by an indirect approach of measuring the general mucoadhesion (film versus a buffered suspension of mucin) and the unspecific adhesion (film versus buffer) for each film formulation. By subtracting the unspecific adhesion (caused by the wetting of the polymer and its subsequent interaction with the filter paper) from the general mucoadhesion, it can be assumed that an estimate of the pure mucin interaction (EMI) was obtained. The mucin interaction of a reference film was compared to films prepared with SLNs using the "coating"

method. The correlation between F_{max} (N) and AUC (N × mm) was good, and therefore only the peak forces of adhesion (F_{max}) are reported in Fig. 2 and analysed further.

The reference film began to disintegrate during the 100 s spent in contact with the moist filter papers, whilst the SLN-loaded films all stayed intact. The addition of SLNs to the film matrix led to a small decrease in the general mucoadhesion and the EMI was not statistically different ($p > 0.05$ for both). Since the reduced ability to adhere to surfaces was not reflected in the films' ability to form bonds with mucin, the overall performance of the film might not be compromised but further investigation is needed.

3.3. Cell studies

Cell studies were performed on monolayers of differentiated HT29-MTX cells. These are often used when mucus is taken into consideration in the assessment of the mucoadhesion, biocompatibility and permeability. The HT29 cell line is a continuous line of human colorectal adenocarcinoma cells. Upon culturing for several passages in medium containing 10^{-6} M methotrexate, the HT29 cells mutated into a new cell line, HT29-MTX, which postconfluently (after approximately 7 days of culturing when seeded at optimal density) differentiate into mucus-secreting goblet cells. This mutation and the goblet-cell characteristics of HT29-MTX cells persisted even after the cell line was cultured further in a methotrexate-free medium (Lesuffleur et al., 1990).

3.3.1. Mucoadhesion

In order to elucidate the advantages of the mucoadhesive formulation, mucoadhesive properties of the developed film formulation (F6) were investigated and compared to the ability of the SLNs themselves to remain attached to the mucus layer of confluent HT29-MTX cells. It is seen from Fig. 3 that a dry, intact film is necessary to allow the polymer and mucin to obtain an intimate surface contact upon swelling, followed by interpenetration and bonding of the HPMC and mucin chains, leading to film mucoadhesion. The mucoadhesion was only slightly reduced after washing, indicating a potential for long-lasting mucoadhesion as well. The initial mucoadhesion diminished when the film was pre-dissolved. It is noteworthy that the pre-dissolved film was not more

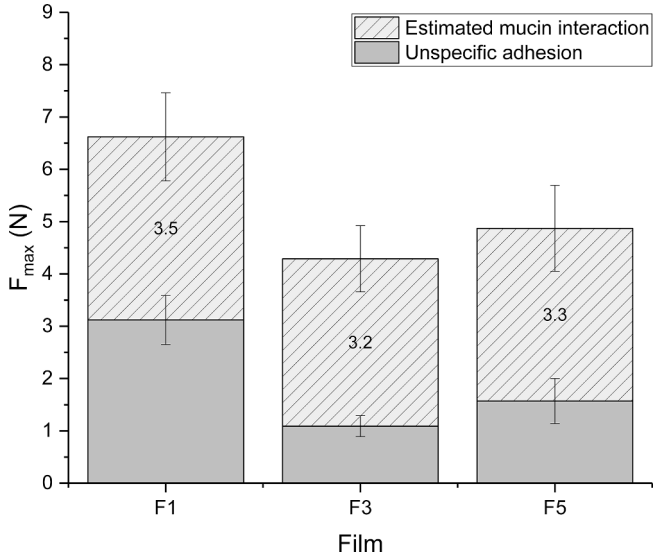

Fig. 2. A graphical representation of the peak forces of adhesion (F_{max}), obtained from the *in vitro* mucin interaction test for the films and the estimated mucin interaction (EMI = general mucoadhesion – unspecific adhesion). Total column height represents the general mucoadhesion. Error bars showing SD (n = 10). No statistical significance (i.e. $p > 0.05$) between EMI of the different formulations was found.

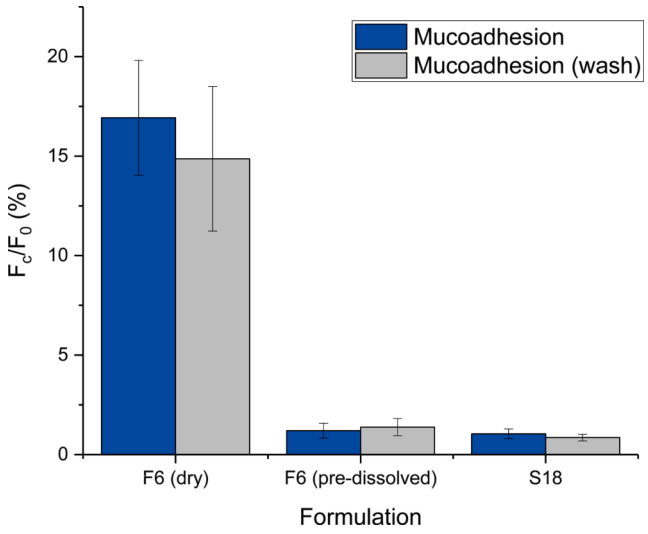

Fig. 3. Normalized FI from direct measurements on cell monolayers after incubation with the different formulations (Mucoadhesion = F_{C1}/F_0) and after cell monolayer was washed with HBSS (Mucoadhesion (wash) = F_{C2}/F_0). Results are expressed as the mean of several measurements with SD calculated using error propagation theory (n = 3 – 5).

diluted than the dry film and this cannot be the reason for the weaker adhesion observed. Under the conditions of the experiment, in the one-hour incubation time, the initial dry film might have contributed to keeping the nanoparticles in close proximity to the mucosal cellular surface. In contrast, the pre-dissolved film had completely lost its original network and the nanoparticles, as well as the polymer chains, were most probably floating in the buffer solution. A potential scenario that HPMC could function as a coating on the SLN surface maintaining mucoadhesion (Luo et al., 2015) for the pre-dissolved sample, could therefore not be confirmed.

The overall low mucoadhesion of the particulate formulation (Fig. 3) was expected, as the particles possess no charge and were not coated with a mucoadhesive component remaining attached to their surface. This formulation can therefore be regarded as a control. The minor adhesion observed is probably of the general kind and not a genuine mucoadhesion. A study on the mucoadhesive properties of different liposomal formulations compared the mucoadhesiveness of differently charged coated and uncoated particles using the same method. The results showed low mucoadhesion for the neutral species consisting only of phospholipids (similar to the SLNs) (Adamczak et al., 2016), consistent with our study. The surfactant component in the SLNs (PS80) is not expected to have any mucoadhesive properties.

3.3.2. Toxicity and permeability studies

The permeability of C6 from different formulations – a C6 suspension (C6-in-HBSS), an SLN suspension (S9-C6-L and S9-C6-H) and film formulation (F6) – through a monolayer of mucus-producing cells was investigated. Assessing the biocompatibility of film formulations is essential already at early stages of the development. Therefore, we chose to combine the permeability study with an examination of the toxicity of each of these formulations on the cell monolayer by measuring monolayer intactness prior to and after incubation with the formulation(s) of interest, by means of TEER-values and CF permeability through the monolayer.

The cells were cultured for 21 – 23 days before the experiments were carried out. The TEER values were measured to be 160 – 250 Ω × cm^2 after deducting blank values. These values were considered acceptable as they approach TEER values reported in the literature of about 200 – 300 Ω × cm^2 for confluent, differentiated HT29-MTX monolayers prior to experiments (Roque et al., 2018). Furthermore, studies have shown

that maximal mucus production and TEER is achieved 23 days after seeding, and 3 weeks is a standard growing period before experiments can be conducted (Pontier et al., 2001; Roque et al., 2018).

C6 – both free and incorporated in SLNs – has earlier been shown to have low toxicity on human epithelial cells (Rivolta et al., 2011). However, the toxicity of the marker itself was not of interest for the current study and in evaluating the toxicity of the formulations, the C6-in-HBSS suspension was used as a control. After incubation with C6-in-HBSS suspension, TEER varied from 125 to 220 Ω × cm^2. Cell monolayers incubated with actual formulations displayed TEER values in the same range for S9-C6-L and F6, and no additional toxicity (neither caused by the moderate concentration of nanoparticles, nor the film polymer themselves) was observed upon examination of TEER-value changes. The TEER values recorded for the cell monolayers incubated with S9-C6-H were in the slightly lower range of 90 – 155 Ω × cm^2, probably due to the approximately tenfold higher concentration of C6 present rather than the formulation excipients themselves. These findings were further supported by the amount of CF permeated, which was highest (2.1%) for one of the monolayers incubated with S9-C6-H, while the CF permeation was otherwise less than 2%. CF is a hydrophilic substance that permeates monolayers through the paracellular route. Increased permeation after exposure to the formulation would mean that the cell monolayer has lost some of its integrity and become leakier. Together with only small drops in TEER values, the minor changes in CF permeability indicate that the SLN formulation (S9-C6) is biocompatible, as supported by the literature (Geszke-Moritz and Moritz, 2016), also at higher concentrations (S9-C6-H), as well as when loaded in the mucoadhesive films.

The expected outcome of the permeability study was a superior permeation of C6 encapsulated in SLNs over the free-C6 suspension and an even further increase in P_{app} for the nanoparticles incorporated into a film matrix. The results, as presented in Fig. 4, show this to be partially the case. The encapsulation of C6 into SLNs had a negative effect on the permeability rate of C6, presumably due to strong association of the hydrophobic substance with the lipid nanoparticles. Interestingly, a study Rivolta *et al.* reports an increased rate of intracellular C6 accumulation when the compound was loaded in SLNs, compared to free C6 and suggests the nanoparticle are not taken up intact into the cells (endocytosis is not the primary entry mechanism) (Rivolta et al., 2011). However, this work was performed on alveolar epithelial cells and the results – obtained in the absence of mucus. Therefore, it is reasonable to suggest that the nanoparticles might have been filtered by the mucus layer due to their size (Larhed et al., 1998; Leal et al., 2017). Further, the nanoparticles could simply have been floating in the buffer during incubation, which made their interaction with the cell membranes a game of chance. The rate of permeation of C6, expressed as the flux (*J*), was increased upon increasing the concentration of nanoparticles present (S9-C6-H). The flux value says something about the rate at which a compound (C6) transverses a membrane of a given area (cm^2), independent of the initial concentration in the donor compartment.

The reduction in P_{app} was compensated for when the particles were loaded into the mucoadhesive film. The advantage of bioadhesive formulations is precisely their ability to achieve a prolonged adherent contact with the mucosa, maintaining an intimate contact with it, which favours drug absorption by creating a high local concentration gradient. The high apparent permeability for the C6-in-HBSS suspension can also be explained by a concentration gradient-driven phenomenon, caused by the fact that the fluorescent probe existed as a suspension, i.e. precipitated onto the cell monolayer.

The magnitude of the calculated P_{app} values presented in Fig. 4a) is comparable to earlier reported values for hydrophobic drugs of similar size (e.g. dexamethasone and other steroids) across a monolayer of Caco-2 cells and are even somewhat higher (Artursson and Karlsson, 1991; Beig et al., 2013). This is surprising since one would expect the mucus layer covering the cell monolayer to be a barrier for the permeability.

3.4. General discussion

In the present study, SLNs with different compositions of soy-phosphatidylcholine (Lipoid S100) and a surfactant (polysorbate 80)

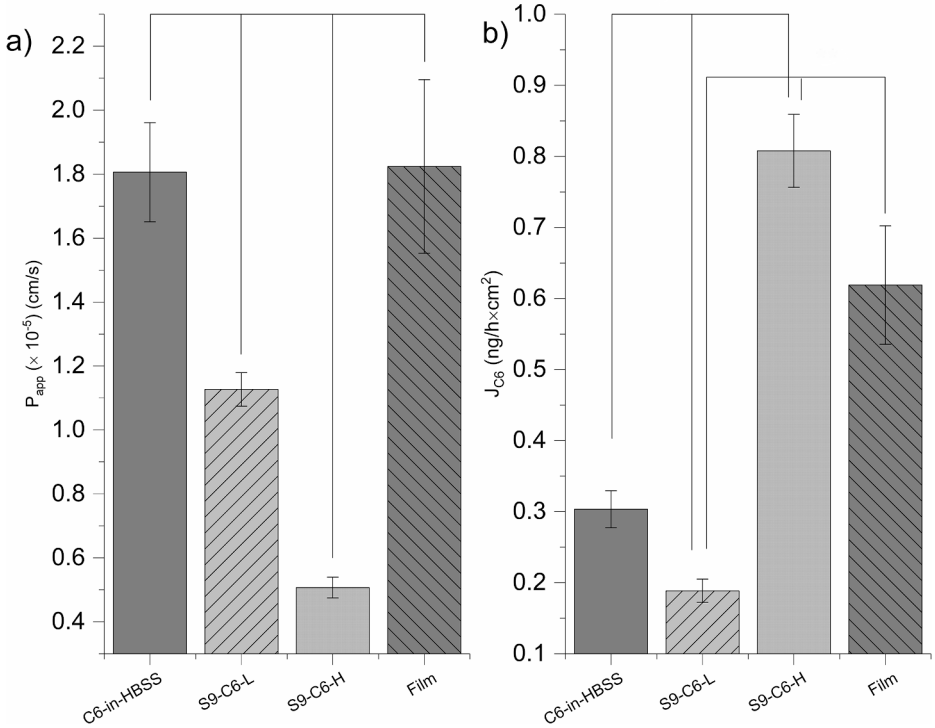

Fig. 4. a) Average apparent permeability coefficients, P_{app} (cm/s) and **b)** average flux values, J_{C6} (ng/cm^2 × h) of C6 across a HT29-MTX cell monolayer, for the tested formulations (where $C_{S9\text{-}C6\text{-}H} = 10 \times C_{S9\text{-}C6\text{-}L}$). Error bars show SD (n = 3). Formulations encompassed by a common bracket are significantly different from each other (α = 0.05).

were successfully prepared by the solvent-injection method both as "placebo" formulations and loaded with the fluorescent probe C6, a model substance with low water solubility. The solvent injection method for preparing SLN is a low-energy method, yielding nanoparticles of good storage stability for at least four months. The hydrodynamic diameter (z-average) of all formulations was within the range of 100 – 200 nm and the PdI around 0.1, both attributes considered satisfactory and the method – robust. The loading with C6 did not contribute to a significant change in either parameter, and the evaporation of methanol did not compromise the formulations. Amongst the investigated formulation and production variables, the main determinants of SLN size were found to be both the lipid and surfactant concentration, as revealed by the optimization CCD-like design.

Different concentrations of SLNs – with and without C6 – were loaded into HPMC-based films. The loaded films exhibited altered properties, as expected, but the differences were, for the most part insignificant and did not reduce the overall quality of the film. The SLN-loaded films showed satisfactory uniformity of mass and thickness, and mechanical strength, flexibility and disintegration were all comparable to the reference films. The mucin interaction of SLN-loaded films was shown to be no less than that of a reference film, indicating that the presence of nanoparticles did not have a deleterious effect on the mucoadhesiveness of the formulation. The mucoadhesive properties of the films were also confirmed in an *in vitro* cell-based test, which also suggested that the particles themselves did not exhibit any mucoadhesive properties. The formulations were found to be biocompatible, even at increased concentrations.

Comparative permeability studies, utilizing the mucus-secreting cell line, showed that the encapsulation of C6 in SLNs had a negative effect on the rate and extent of permeation. This negative effect was counteracted by inclusion of the SLN into a mucoadhesive film, which achieved a higher rate and degree of permeability. This indicates the importance of an intact mucoadhesive film for the satisfactory *in vivo* permeability of a drug solubilized in SLNs. This knowledge is important to assure that a suitable disintegration time of the film matrix is aimed for during development and the composition altered accordingly. Our results indicate that the disintegration time should be aligned with the rate of permeability of the relevant drug.

However, these *in vitro* results are not directly transferrable to the *in vivo* situation. For instance, the composition of mucus and ionic strength may differ, both of which influences the hydration and viscoelastic properties of mucus (Leal et al., 2017). Solvent volumes and mechanical stress that the formulation has to tolerate *in vivo* have not been mirrored. The incubation conditions, somewhat standard for cell experiments, are quite far from the *in vivo* situation, e.g. with respect to the role gravity plays in keeping the formulation in contact with the cell monolayer. However, when developing new formulations, *in vitro* methods offer an invaluable opportunity for comparing different potential candidates. The experiments have been a tool in an attempt to evaluate the advantage of loading SLNs into a mucoadhesive film.

The transition to an API will increase the clinical relevance of this work and would naturally require separate thorough optimization of formulation and production parameters. It is expected that the encapsulation of an API into SLNs would prevent it from coming into contact with the taste receptors in the oral cavity and, thus, provide a superior taste masking (Walsh et al., 2014), but this needs to be assessed at a later stage of the formulation development. Furthermore, drug release – rate and extend – from the nanoparticles is of great importance once working with an actual API.

4. Conclusions

In conclusion, this project explored simple and inexpensive, yet robust methods for the preparation of monodisperse nanoparticles and of thin polymeric films, loaded with these. The results managed to show that it has the potential to be developed into a successful mucoadhesive film formulation containing a poorly water-soluble drug.

CRediT authorship contribution statement

Martina M. Tzanova: Methodology, Formal analysis, Investigation, Writing - original draft, Visualization. **Ellen Hagesaether:** Methodology, Writing - review & editing, Supervision. **Ingunn Tho:** Conceptualization, Methodology, Resources, Writing - review & editing, Supervision, Project administration.

Declaration of Competing Interest

The authors declare that they have no known competing financial interests or personal relationships that could have appeared to influence the work reported in this paper.

Acknowledgements

Thanks to Lipoid GmbH, DE for generously supplying the Lipoid S100, to professor Tor Gjøen for the access to the plate reader and to our lab technicians, Bente Breiby, Ivar Grove and Tove Larsen. The cell line HT29-MTX was kindly provided by Dr. Thécla Lesuffleur (INSERM UMR S 938, Paris, FR).

Funding

This research did not receive any specific grant from funding agencies in the public, commercial, or not-for-profit sectors.

References

Abd El Azim, H., Nafee, N., Ramadan, A., Khalafallah, N., 2015. Liposomal buccal mucoadhesive film for improved delivery and permeation of water-soluble vitamins. Int. J. Pharm. 488, 78–85.

Adamczak, M.I., Hagesæther, E., Smistad, G., Hiorth, M., 2016. An in vitro study of mucoadhesion and biocompatibility of polymer coated liposomes on HT29-MTX mucus-producing cells. Int. J. Pharm. 498, 225–233.

Adrover, A., Varani, G., Paolicelli, P., Petralito, S., Di Muzio, L., Casadei, M.A., Tho, I., Adrover, A., 2018. Experimental and Modeling Study of Drug Release from HPMC-Based Erodible Oral Thin Films. Pharmaceutics. 10.

Alopaeus, J.F., Hellfritzsch, M., Gutowski, T., Scherließ, R., Almeida, A., Sarmento, B., Škalko-Basnet, N., Tho, I., 2020. Mucoadhesive buccal films based on a graft co-polymer – A mucin-retentive hydrogel scaffold. Eur. J. Pharm Sci. 142.

Artursson, P., Karlsson, J., 1991. Correlation between oral drug absorption in humans and apparent drug permeability coefficients in human intestinal epithelial (Caco-2) cells. Biochem. Biophys. Res. Commun. 175, 880–885.

Beig, A., Agbaria, R., Dahan, A., Beig, A., 2013. Oral delivery of lipophilic drugs: The tradeoff between solubility increase and permeability decrease when using cyclodextrin-based formulations. PLoS ONE 8, e68237.

Biomedicals, M., Technical information: Coumarin 6. MP Biomedicals.

Douroumis, D., Fahr, A., 2012. Drug delivery strategies for poorly water-soluble drugs. John Wiley & Sons, Chichester, West Sussex.

Edgar, M., Dawes, C., O'Mullane, D., 2012. Factors Influencing Salivary Flow Rate and Composition, in: Dawes, C. (Ed.), Saliva and oral health : an essential overview for the dental professional, 4 ed. [reprinted 2015]. ed. Stephen Hancocks Ltd, Duns Tew, Great Britain, pp. 37-55.

Esbensen, K.H., Guyot, D., Westad, F., Houmøller, L.P., Camo, A.S.A., 2001. Multivariate data analysis - in practice : an introduction to multivariate data analysis and experimental design, 5th ed. Camo, Oslo.

European Medicines Agency, 2006. Regulation (EC) No 1901/2006 of the European Parliament and of the Council of 12 December 2006 on medicinal products for paediatric use and amending Regulation (EEC) No 1768/92, Directive 2001/20/EC, Directive 2001/83/EC and Regulation (EC) No 726/2004, Official Journal of the European Union, p. 19.

European Pharmacopoeia Commission, 2018. 2.9.5. Uniformity of mass of single-dose preparations. Strasbourg, France: European Directorate for the Quality of Medicines (EDQM), In: European Pharmacopoeia. 9th edition., pp. 4787-4790.

Finke, J.H., Richter, C., Gothsch, T., Kwade, A., Büttgenbach, S., Müller-Goymann, C.C., 2014. Coumarin 6 as a fluorescent model drug: How to identify properties of lipid colloidal drug delivery systems via fluorescence spectroscopy? Eur. J. Lipid Sci. Technol. 116, 1234–1246.

Geszke-Moritz, M., Moritz, M., 2016. Solid lipid nanoparticles as attractive drug vehicles: Composition, properties and therapeutic strategies. Mater. Sci. Eng., C 68, 982–994.

Giovino, C., Ayensu, I., Tetteh, J., Boateng, J.S., 2013. An integrated buccal delivery system combining chitosan films impregnated with peptide loaded PEG-b-PLA nanoparticles. Colloids Surf. B 112, 9–15.

Gordillo-Galeano, A., Mora-Huertas, C.E., 2018. Solid lipid nanoparticles and nanostructured lipid carriers: A review emphasizing on particle structure and drug release. Eur. J. Pharm. Biopharm. 133, 285–308.
Hagesaether, E., Hiorth, M., Sande, S.A., 2009. Mucoadhesion and drug permeability of free mixed films of pectin and chitosan: An in vitro and ex vivo study. Eur. J. Pharm. Biopharm. 71, 325–331.
Hazzah, H.A., Farid, R.M., Nasra, M.M.A., El-Massik, M.A., Abdallah, O.Y., 2015. Lyophilized sponges loaded with curcumin solid lipid nanoparticles for buccal delivery: Development and characterization. Int. J. Pharm. 492, 248–257.
Jones, E., Ojewole, E., Kalhapure, R., Govender, T., 2014. In vitro comparative evaluation of monolayered multipolymeric films embedded with didanosine-loaded solid lipid nanoparticles: a potential buccal drug delivery system for ARV therapy. Drug Dev. Ind. Pharm. 40, 669–679.
Karki, S., Kim, H., Na, S.-J., Shin, D., Jo, K., Lee, J., 2016. Thin films as an emerging platform for drug delivery. Asian J. Pharm. Sci. 11, 559–574.
Kim, S., Traore, Y.L., Lee, J.S., Kim, J.H., Ho, E.A., Liu, S., 2017. Self-assembled nanoparticles made from a new PEGylated poly(aspartic acid) graft copolymer for intravaginal delivery of poorly water-soluble drugs. J. Biomater. Sci. Polym. Ed. 28, 2082–2099.
Krampe, R., Visser, J.C., Frijlink, H.W., Breitkreutz, J., Woerdenbag, H.J., Preis, M., 2016. Oromucosal film preparations: points to consider for patient centricity and manufacturing processes. Expert Opin. Drug Deliv. 13, 493–506.
Larhed, A., Artursson, P., Björk, E., 1998. The Influence of intestinal mucus components on the diffusion of drugs. An Official J. Am. Association Pharmaceutical Sci. 15, 66–71.
Leal, J., Smyth, H.D.C., Ghosh, D., 2017. Physicochemical properties of mucus and their impact on transmucosal drug delivery. Int. J. Pharm. 532, 555–572.
Lesuffleur, T., Barbat, A., Dussaulx, E., Zweibaum, A., 1990. Growth adaptation to methotrexate of HT-29 human colon carcinoma cells is associated with their ability to differentiate into columnar absorptive and mucus-secreting cells. Cancer Res. 50, 6334–6343.
Leyva-Gómez, G., Piñón-Segundo, E., Mendoza-Muñoz, N., Zambrano-Zaragoza, M., Mendoza-Elvira, S., Quintanar-Guerrero, D., 2018. Approaches in polymeric nanoparticles for vaginal drug delivery: A review of the state of the art. Int. J. Mol. Sci. 19, 1549.
Luo, Y., Teng, Z., Li, Y., Wang, Q., 2015. Solid lipid nanoparticles for oral drug delivery: Chitosan coating improves stability, controlled delivery, mucoadhesion and cellular uptake. Carbohydr. Polym. 122, 221–229.
Martins, S., Tho, I., Souto, E., Ferreira, D., Brandl, M., 2012. Multivariate design for the evaluation of lipid and surfactant composition effect for optimisation of lipid nanoparticles. Eur. J. Pharm. Sci. 45, 613–623.
Mazzarino, L., Borsali, R., Lemos-Senna, E., 2014. Mucoadhesive films containing chitosan-coated nanoparticles: A new strategy for buccal curcumin release. J. Pharm. Sci. 103, 3764–3771.
Mortazavian, E., Dorkoosh, F.A., Rafiee-Tehrani, M., 2014. Design, characterization and ex vivo evaluation of chitosan film integrating of insulin nanoparticles composed of thiolated chitosan derivative for buccal delivery of insulin. Drug Dev. Ind. Pharm. 40, 691–698.
Musazzi, U.M., Dolci, L.S., Albertini, B., Passerini, N., Cilurzo, F., 2019. A new melatonin oral delivery platform based on orodispersible films containing solid lipid microparticles. Int. J. Pharm. 559, 280–288.
Pontier, C., Pachot, J., Botham, R., Lenfant, B., Arnaud, P., 2001. HT29-MTX and Caco-2/TC7 monolayers as predictive models for human intestinal absorption: Role of the mucus layer. J. Pharm. Sci. 90, 1608–1619.
Preis, M., Knop, K., Breitkreutz, J., 2014. Mechanical strength test for orodispersible and buccal films. Int. J. Pharm. 461, 22–29.
Rivolta, I., Panariti, A., Lettiero, B., Sesana, S., Gasco, P., Gasco, M., Masserini, M., Miserocchi, G., 2011. Cellular uptake of coumarin-6 as a model drug loaded in solid lipid nanoparticles. J. Physiol. Pharmacol. 62, 45–53.
Roque, L., Alopaeus, J., Reis, C., Rijo, P., Molpeceres, J., Hagesaether, E., Tho, I., Reis, C., 2018. Mucoadhesive assessment of different antifungal nanoformulations. Bioinspiration Biomim. 13, e055001–e55010.
Schubert, M.A., Müller-Goymann, C.C., 2003. Solvent injection as a new approach for manufacturing lipid nanoparticles – evaluation of the method and process parameters. Eur. J. Pharm. Biopharm. 55, 125–131.
Speer, I., Steiner, D., Thabet, Y., Breitkreutz, J., Kwade, A., 2018. Comparative study on disintegration methods for oral film preparations. Eur. J. Pharm. Biopharm. 132, 50–61.
Ternullo, S., de Weerd, L., Holsæter, A.M., Flaten, G.E., Škalko-Basnet, N., 2017. Going skin deep: A direct comparison of penetration potential of lipid-based nanovesicles on the isolated perfused human skin flap model. Eur. J. Pharm. Biopharm. 121, 14–23.
Walsh, J., Cram, A., Woertz, K., Breitkreutz, J., Winzenburg, G., Turner, R., Tuleu, C., 2014. Playing hide and seek with poorly tasting paediatric medicines: Do not forget the excipients. Adv. Drug Deliv. Rev. 73, 14–33.